Characterization of the Organic and Inorganic Supercapacitors

Ana-Maria MUŞAT[1, 2], Radu MUŞAT[1, 3], Marius CARP[1, 2], Paul BORZA[1], Gerard COQUERY[4]
Transylvania University of Braşov[1], Siemens PSE SRL Braşov Romania[2], IBM Romania[3], Institut français des sciences et technologies des transports, de l'aménagement et des réseaux[4]
ana_maria.puscas@yahoo.com, r_musat@yahoo.com, marius.carp@yahoo.com, paul.borza@unitbv.ro, gerard.coquery@ifsttar.fr

***Abstract* - The aim of the paper is to emphasize the differences between the behavior of the organic and inorganic supercapacitors in order to obtain a good understating of their optimal applications. The differences were obtained and determined while testing two types of supercapacitors with cycling temperature, DC charge discharge and electric impedance spectroscopy procedures. To anticipate the behavior of such devices in applications of electric vehicles and hybrid electric vehicles, the corresponding models were necessary to be determined. The testing procedures were necessary for determining the values of the parameters used in the modeling process and for validating the developed electric models. In the present paper, the results of the experiments were interpreted, the specific parameters were identified and the electrical models were determined.**

I. INTRODUCTION

In designing process of a modern vehicle, a strong inter-correlation between inputs, outputs and constraints can be identified. This dependency is illustrated in Fig. 1, as it follows: the inputs represent the energy accumulated into the storage devices; the outputs have to guarantee the system's requirements and performances; the constraints are related to the weigh of the system, the dynamics, the operating temperature range, pollution etc.

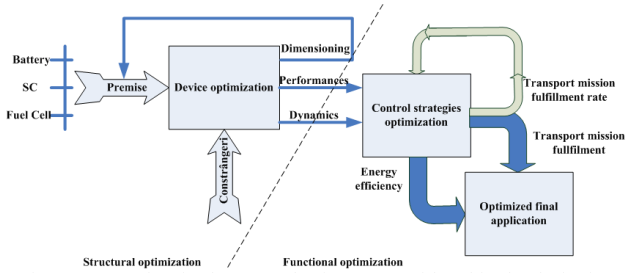

Fig. 1. Dependencies between the factors considered in the designing process of a vehicle.

From Fig. 1, a strong correlation between all the factors considered in the vehicle's designing and sizing phases can be identified. The performances of a vehicle are influenced both by the storage devices and by the control strategies used in the process of optimizing the energy flow. The control strategies are implemented to optimally correlate the inputs and the constraints, thus to increase the energy efficiency of the final application.

In the last years, great attention has been given to developing and improving the technology of the electric vehicles (EV) and hybrid electric vehicles (HEV) by improving their energy storage devices. The main storage and generation devices (SGD) used in automotive are: batteries, supercapacitors (SC), flywheels and fuel cells. Unfortunately, the actual SGD limit the autonomy and the dynamics of the vehicles and have a negative impact on the environment. Thus, research studies are focused on combining different devices to create hybrid energy storage devices able to ensure both energy density and power density with high efficiency. The above mentioned devices are used especially because of their complementary performances related to energy and power density, time constants, life cycle, operating temperature and frequency. To obtain devices with selectable variable time constant, increased energy and power density, increased life time and stability over a wide range of temperatures, the technology of the storage and generation devices is continuously improving.

The Ragone diagram (Fig. 2) provides a synthetic image on the power and energy density and facilitates the sizing process of the final application. While considering the experimentally determined specific behavior of the storage and generation device, the load requirements can be harmonized with the energy generator ones, in order to increase the energy efficiency of the storage and generation processes.

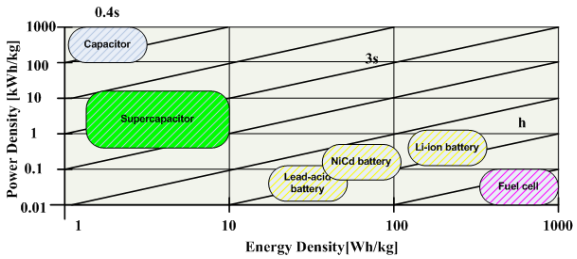

Fig. 2. Ragone Diagram.

As it can be seen from Fig. 2, the performances of the supercapacitors complement the ones of the batteries and of the dielectric capacitors by ensuring power density together with energy density. Such behavior can be useful especially in HEV and EV.

To increase the energy efficiency and the performances of the final application (HEV or EV), combined energy storage devices are researched and implemented. A combined energy

storage device is composed of storage and generation devices with different performances (energy density, power density, time constants), electrical switches for connecting the storage devices and embedded control systems able to intelligently control the topology of the devices, thus to ensure the optimal load profile [1]. The connection type is selected by the control system based on an intelligent microcontroller, which anticipates the behavior of the application, predicted by the results of the electrical model simulation [1]. To ensure optimal performances for such a hybrid device, the electrical characteristics of the used storage and generation devices has to be identified.

The goal of the present paper is to identify and model the behavior of the supercapacitors, to compare the performances between two types of supercapacitors (organic and inorganic) and to identify the corresponding electrical models.

II. ORGANIC VS. INORGANIC SUPERCAPACITORS

A supercapacitor is an electrochemical capacitor, characterized by small time constants and composed of load collector, porous electrodes, electrolyte and separator made from porous material with increased purity (Fig. 3) [2].

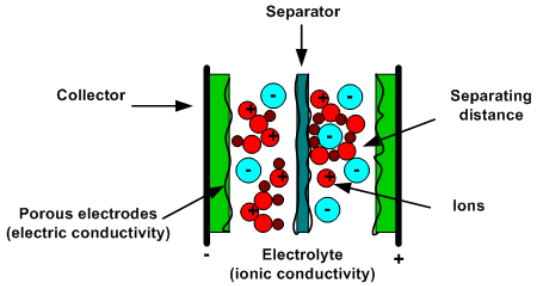

Fig. 3. Supercapacitor – Internal Structure.

The *porous electrodes* are made from material like activated carbon, metallic oxides (RuO_2, IrO_2), polymers etc. Depending on the *electrolyte*, supercapacitors can be grouped in two categories: organic and inorganic. The organic electrolyte (organic solvents - acetonitryl) ensures a good mobility of the ions, even at reduced temperatures [3]. Its disadvantages are related to the risk of explosion while working at extreme high temperatures ($> 70\ ^oC$). The disadvantage of the inorganic electrolyte (H_2SO_4 or KOH) is related to the nominal cell voltage level (0.7 V ÷ 1.5 V), which is more reduced than in the organic electrolyte case (2.5 V ÷ 3.5 V). The advantage of the inorganic electrolyte is related to extending the positive temperature range, thus reducing the risk of explosion [4], [5]. Additionally, the inorganic electrolyte is characterized by increased value of the conductivity (0.8 S / cm ÷ 1 S / cm for H_2SO_4) [6] than in the case of the organic one (0.02 S / cm ÷ 0.05 S / cm) [7], [8], [9].

By comparing the two types of supercapacitors, it can be identified that the organic supercapacitor is characterized by high specific energy and the inorganic one by high specific power, and increased life cycle [3], [10].

In both cases, the material that composes the electrolyte can introduce severe limitations in terms of performances, they being influenced especially by the temperature and frequency variation.

The *separator* is a porous membrane (paper, glass fiber, polymer) which delimitates the two electric layers of the supercapacitor, insulates the electrodes and ensures the ion transfer between the electrodes by using the electrolyte, which penetrates the pores of the separator. The separator is characterized by small electric series resistance (0.1 mΩ ÷ 100 mΩ), directly proportional with the thickness of the separator (10 ÷ 100 μm) and reversely proportional with its contact surface [6]. Also, the conductivity value of the separator is directly proportional with its porosity [6], [8]. Some of the separators are pure aluminum for organic supercapacitors and stainless steel for inorganic ones [11]. For supercapacitors it can be delimited three main types of pores, depending on their size: micropores (< 2 nm), mezopores (2 nm ÷ 20 nm) and macropores (20 nm ÷ 50 μm) [12], [13]. The pore size influences the energy density, the power density and the capacitance which is increasing while reducing the pore size [14]. The ionic conductivity increases in the case of the pores smaller than 2 nm [4], [14]. On the other hand, the micropores are blocking the ions thus increasing the electric series resistance (*ESR*) value and reducing the maximum value of the power density. Experimentally has been demonstrated that the optimal value of the pore size is less than 1 nm (ultramicropores): 0.7 nm for aqueous inorganic electrolyte and 0.8 nm for organic electrolyte [12], [15].

For identifying the behavior of the supercapacitors used in automotive applications, experiments have to be made and models have to be identified, by using the data records obtained from different testing methods.

III. METHODS FOR TESTING THE ORGANIC AND INORGANIC SUPERCAPACITORS

Automotive applications, especially for EV and HEV are dynamics and thus, identifying the behavior of the SGD used by the application is crucial. At present, the behavior of the SGD used as energy sources in automotive is dependent both on internal factors (material type, chemical reactions) and external factors (temperature, pressure) [16].

A. Testing methods

To determine the behavior of the supercapacitors and to identify their corresponding models, three types of experiments were made: cycling temperature, direct constant current (DC) charge discharge and impedance spectroscopy.

The *cycling temperature* method was used for identifying the leakage current and the thermal stability of the SC.

The *DC charge discharge* method was used to determine the electric series resistance and the capacitance of the supercapacitor. Its advantages are related to the reduced testing time and its disadvantages are related to having no possibility to accurately characterize the transitory chemical processes which appear inside the supercapacitor.

The *electric impedance spectroscopy* (EIS) method was used to accurately characterize the dynamic behavior of the tested SC, the measurement precision not being limited by the relaxing time of the device or by its behavior irregularities [17]. The EIS measurements provide information related to the variation of the parameters of the supercapacitors (such as ESR, capacitance, phase, impedance) with frequency and temperature [18].

For testing, two different types of supercapacitors were chosen: an organic SC prototype (BatScap 2.7 V / 2600 F) and a fully cycled inorganic SC (ECOND 14 V / 40 F).

The experiments were made to determine the variation of the *ESR* and of the capacitance (C_{dl}) with temperature and frequency, parameters which influence the energy and power density. Using the values of the parameters determined with *EIS* method, the corresponding electrical models were determined. Using the DC charge/discharge experimental results, the electrical models were validated.

B. Testing procedures

For testing the organic and inorganic SC, three testing procedures were conceived: cycling temperature, DC charge/discharge and electric impedance spectroscopy.

BI. The ***cycling temperature procedure*** consists in maintaining the nominal voltage level constant at the SC terminals, varying the temperature (as it is illustrated in Fig. 4) and monitoring the value of the leakage current. The inorganic SC was tested during a 34 hours cycle and the current value was monitored through a 10 Ω power resistor.

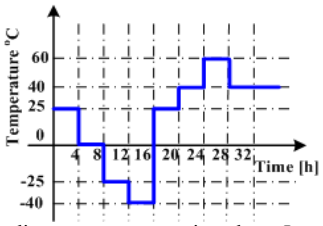

Fig. 4. Cycling temperature testing plan – Inorganic SC.

The testing procedures (DC charge/discharge – Fig. 3 and EIS – Fig. 4.) were defined together with the research team from IFSTTAR (Institut français des sciences et technologies des transports, de l'aménagement et des réseaux), taking into consideration the IEC 62391 standard from 2006 [19], [20], [21]. To obtain accurate experimental results, thermal stabilization was required before testing: 2 hours for organic SC and 4 hours for inorganic SC.

BII. The ***DC charge/discharge*** **procedure** is illustrated in Fig. 5.

The testing procedure consisted of four stages: charging, chemical stabilization, discharging and relaxing. The charging process was made at constant current (I_c = 5 mA) to a preset threshold value (U_{th} = 2.7 V for organic SC and U_{th} = 14 V for inorganic SC). The charging process was followed by a stabilization period (t_s = 30 minutes) and by a discharging period (t_d = 5 s) at constant current (I_d = 100 mA / F). In the discharging process the voltage variation was monitored at the SC terminals.

For determining the *ESR* value using (1), the voltage at the end of the discharging process (U_1) and the voltage after 5 seconds of relaxation (U_2) were considered [22].

$$ESR = \frac{U_2 - U_1}{I_d} \tag{1}$$

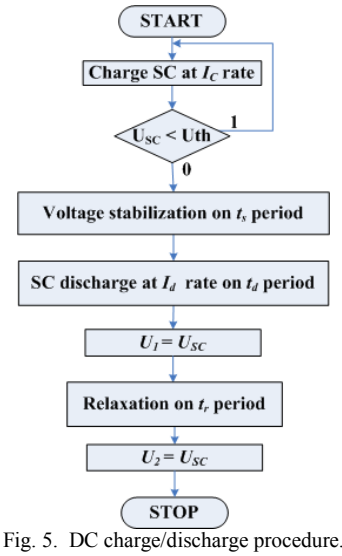

Fig. 5. DC charge/discharge procedure.

The value of the capacitance was determined by using (2) and (3):

$$C = \frac{I \cdot \Delta t}{\Delta U_{cap}}. \tag{2}$$

$$\Delta U_{cap} = (0.8 \cdot U_{th} - 0.4 \cdot U_{th}) - (0.6 \cdot U_{th} - 0.3 \cdot U_{th}) \tag{3}$$

where ΔU_{cap}: voltage drop in the discharging process.

BIII. The ***EIS procedure*** (Fig. 6) was used to determine the variation of the electrical impedance ($Z(\omega)$) on a preset frequency range by applying a small AC voltage signal ($U(\omega)$ = 100 mV (4)) at the charged SC terminals and measuring the current variation ($I(\omega)$ (5)). The SC was pre-charged at the nominal voltage level (2.7 V for organic SC and 14 V for inorganic SC) and stabilized: 2 hours for organic SC and 4 hours for inorganic SC.

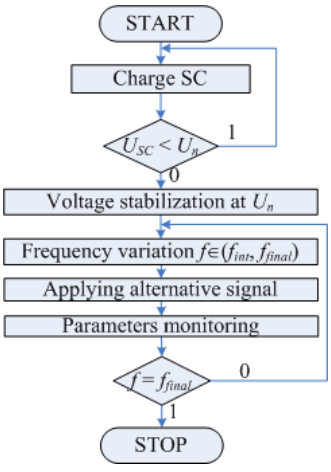

Fig. 6. EIS procedure.

where $U(\omega) = U_0 \cdot e^{j \cdot \omega \cdot t}$ (4)

and $I(\omega) = I_0 \cdot e^{j \cdot (\omega \cdot t - \varphi)}$ (5)

The value of the electric impedance ($Z(\omega)$) is determined using (6):

$$Z(\omega) = U(\omega) / I(\omega) = Z_0 \cdot e^{j \cdot \varphi} \quad (6)$$

The Bode and Nyquist diagram and also the real and imaginary part were determined by using IM6 device and *Thales* software.

The *ESR* value was determined where the behavior of the SC became resistive ($Im(Z) = 0$). For determining the capacitance value (C_{dl}), the experimental data, (3) and (7) were used [23].

$$C(f) = \begin{cases} -\dfrac{1}{2 \cdot \pi \cdot f} \cdot \mathrm{Im}(Z), f < 1Hz \\ \dfrac{1}{2 \cdot \pi \cdot f} \cdot (2 \cdot \pi \cdot f \cdot L - \mathrm{Im}(Z)), f > 1Hz \end{cases} \quad (7)$$

Additionally, (7) was used for determining the variation of the C_{dl} in the tested range of frequencies.

IV. Experiments and Results

A. Cycling temperature

In the following figures are illustrated the experimental results obtained while testing the SC with cycling temperature procedure in order to determine the behavior (Fig. 7) and the leakage current (Fig. 8) of the stationary tested inorganic SC. In the testing process only the positive temperatures were monitored. The experimental data were processed by using MatlabR2007 tool.

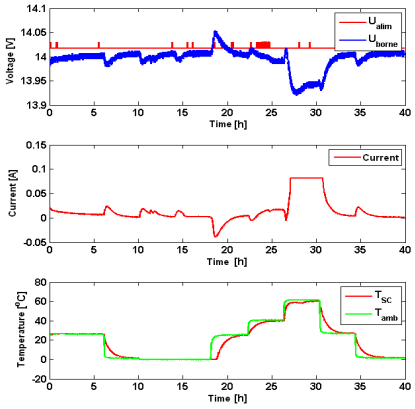

Fig. 7. Cycling temperature – experimental results.

From Fig. 7 it can be identified how the temperature variation influences the voltage and current values. The dependency of the voltage and current with temperature is amplified especially when the temperature increases from 40 °C to 60 °C.

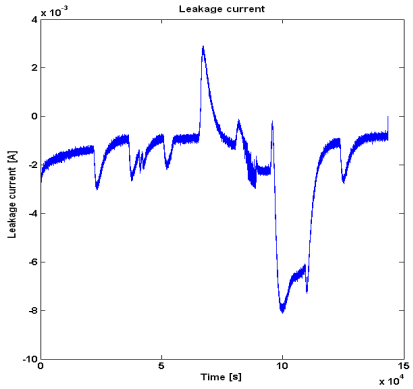

Fig. 8. Leakage current.

From Fig. 8 it can be identified that the leakage current is amplified at extreme high temperatures (60 °C), where the voltage measured at the SC terminals has increased variations. This is due to the dependency between the ionization process of the electrolyte and temperature. Also, from Fig. 8 the time necessary for thermal stabilization of the SC (2 hours for organic SC and 4 hours for inorganic SC) was identified.

B. DC charge/discharge

DC charge/discharge procedure was applied on both types of SC (organic and inorganic) to identify their behavior and to validate their equivalent electric models. The SC were pre-charged and stabilized at their nominal voltage levels (2.7 V for organic SC and 14 V for inorganic SC) and were discharged with 100 mA/F. The experiments were processed in MatlabR2007 tool.

The DC charge/discharge experiments made on the 2.7 V/2600 F organic SC are illustrated in Fig. 9.

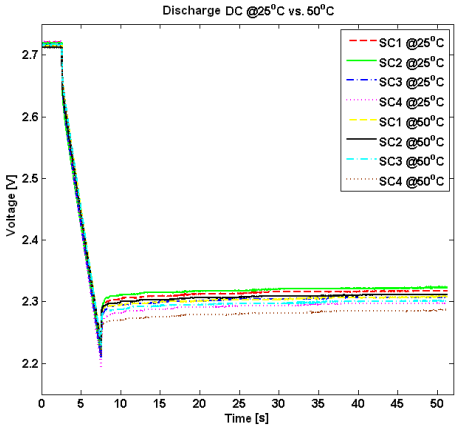

Fig. 9. Organic SC.

The DC charge/discharge experiments made on the 14 V/40 F inorganic SC are illustrated in Fig. 10.

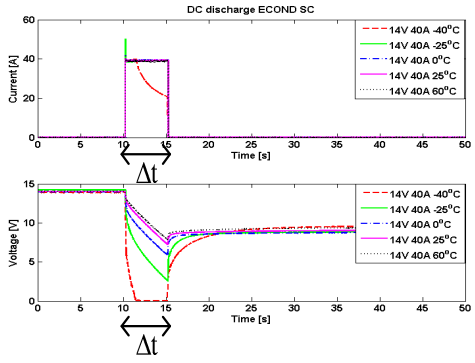

Fig. 10. Inorganic SC.

As it can be seen from the experimental results, the behavior of both types of SC is influenced by the temperature variation, their performances being reduced while decreasing the testing temperature. This disadvantage is emphasized in the case of the inorganic SC because of its internal structure. For determining the resistance variation function of temperature, (8) was used.

$$ESR = R_{25^oC} \cdot (1 + \alpha \cdot (T - t_0)) \quad (8)$$

The *ESR* and C_{dl} variation with temperature of the inorganic SC is illustrated in Fig. 11 and Fig. 12.

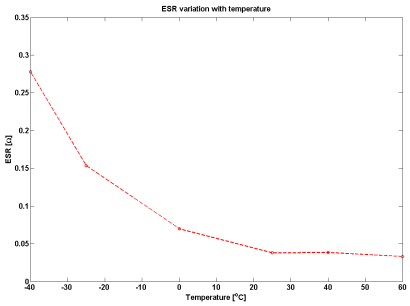

Fig. 11. *ESR* = f (*T*).

For the organic SC, the *ESR* varied with 28.73 % (0.1 mΩ), decreasing from 0.348 mΩ at 25 °C to 0.248 mΩ at 50 °C. In the case of the inorganic SC, the *ESR* decreased from 0.039 Ω at 25 °C to 0.03 Ω at 60 °C, thus varying with 23 %. The variation is more significant at low temperatures, where the value of the ESR increased to 0.278 Ω at - 40 °C.

A significant dependence between the inorganic SC capacitance value and the temperature was identified from Fig. 12.

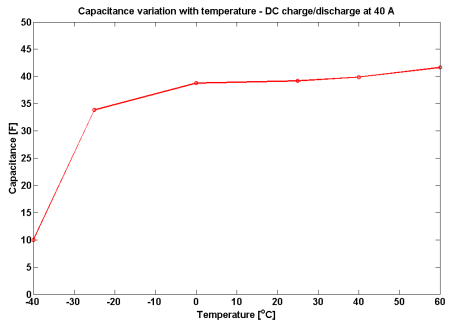

Fig. 12. *C* = f (*T*).

The value of the capacitance increased with 6.2 %, from 39.2 F at 25 °C to 41.63 F at 60 °C. The dependency between capacitance and temperature is more increased at low temperatures, where the capacitance value decreases to 33.83 F at - 25 °C (13.7 %) and to 9.98 F at - 40 °C (74.5 %).

C. Electric Impedance Spectroscopy - EIS

The two types of SC were tested with EIS procedure in order to identify their specific electric parameters necessary in the modeling process: *ESR*, C_{dl}. The results of the experiments are illustrated in Fig. 13 and Fig. 14.

In Fig. 13 there are illustrated the results of the EIS measurements made on the organic SC.

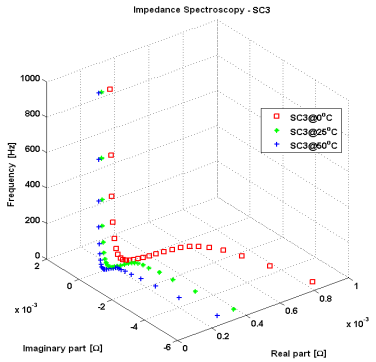

Fig. 13. SC organic: 3D frequency-impedance dependency with temperature.

In Fig. 14 there are illustrated the results of the EIS measurements made on the inorganic SC.

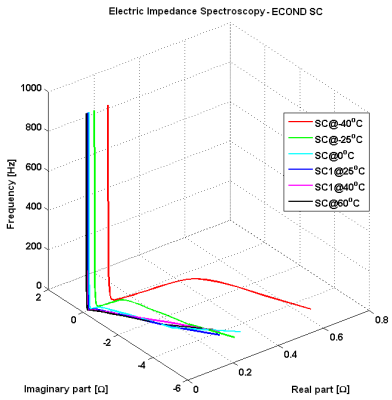

Fig. 14. SC inorganic: 3D frequency-impedance dependency with temperature.

As it can be seen from Fig. 13 and Fig. 14, the behavior of the parameters of both types of SC is influenced by the frequency variation. At reduced frequencies, the real part of the measured electrical impedance has increased values and it is reducing while increasing the testing frequency. The absolute value of the imaginary part of the electrical impedance is reducing with frequency until it reaches 1 Hz.

While operating at extreme temperatures and over-voltages, acceleration of the parasitic electrochemical reaction and electrolyte decomposition were identified. As a result, if the supercapacitors are functioning at temperatures with 10 K more than the nominal temperature and at over-voltages (more than 10 mV over the nominal voltage), their

lifetime is reduced at half [24], [25]. As a consequence, we can state that the testing procedures can influence the behavior of the supercapacitors. For the accuracy of the experiments, together with IFSTTAR team it was decided that strict testing procedures have to be defined for testing both types of supercapacitors.

V. MODELING THE SUPERCAPACITORS

There are multiple research studies focused on developing equivalent electrical models of the supercapacitors [26], [27], [28]. While testing, Zubieta and Bonet delimited two types of phenomena for supercapacitors [27], [28]:

- *Rapid phenomena:* are identified during the DC charging and discharging processes, while the charge is transferred through the electrolyte. This behavior can be modeled by connecting in series the *ESR* with a variable capacitance.
- *Slow phenomena*: are identified during the load redistribution processes and during the relaxation period of the electrochemical device. This behavior can be modeled by using parallel R_iC_i groups characterized by more increased time constants than in the rapid phenomena case, like it is illustrated in Fig. 15.

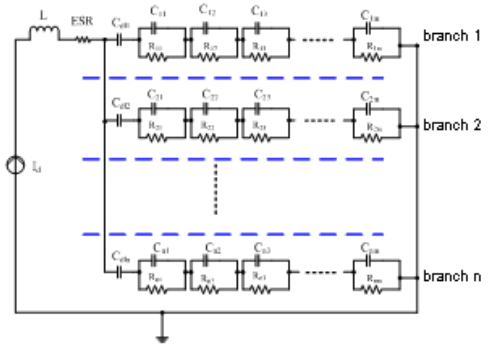

Fig. 15. SC Electric model: n branches, m parallel gruops (Ri,Ci).

The first branch of the model is the predominant one (rapid branch because of the short time constant) $(n = 1) \rightarrow (R_{1j}, Cdl_{1j})$. The supplementary branches $(n > 1)$ are used for increasing the accuracy of the slow phenomena modeling process. Moreover, by increasing the number of the parallel groups $(m > 1)$ the accuracy of the process of modeling the device's energy distribution during the relaxation process can be increased. At the end of the discharging process, the load is concentrated in the first parallel group $(m = 1)$ and after that, during the relaxation process, the load is transferred through the superior groups.

To implement the multiple branches and parallel groups of the electrical models of the supercapacitors, the hypothesis of the time constants has to be respected. This hypothesis states that the superior branches of the electrical model are characterized by time constants more increased than the ones of the inferior branches ($\tau_i+1 >> \tau_i$). Supplementing the number of branches is useful especially in the case of modeling the slow processes identified in the SC. The disadvantage is the complexity, by increasing the difficulty of determining the values of the corresponding specific electric parameters and increasing the processing time.

The parameters (*ESR*, R_i, C_{dl}) of the SC electrical model were determined by using the EIS experimental data. The *ESR* value was determined at pure resistive behavior of the SC ($\mathrm{Im}(Z) = 0$) and the C_{dl} value at low frequency. The DC charge/discharge experimental data were used to identify the accuracy between the simulated model and the experiments and to validate the model. Models with $1 \div 4$ branches were conceived and for error analysis (9) was used:

$$|Error| = \frac{\delta}{V_{\exp}} = \frac{|V_{sim} - V_{\exp}|}{V_{\exp}} \cdot 100\,[\%] \qquad (9)$$

where: V_{sim}: voltage - simulated value;
V_{exp}: voltage -experimental data.

The simulations were made in Orcad simulation tool.

The results of the simulation vs. experiments in the case of the 2.7 V / 2600 F organic BatScap SC are illustrated in Fig. 16 and the error between the model and experiments in Fig. 17.

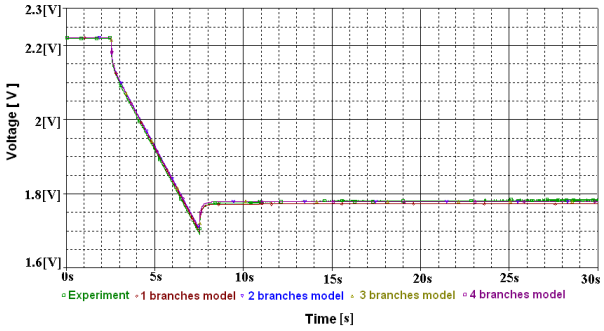

Fig. 16. Organic SC: Simulation vs. Experiment.

From Fig. 16 it can be identified the accuracy of the developed models for the organic SC, this being emphasized in the error analysis (Fig. 17).

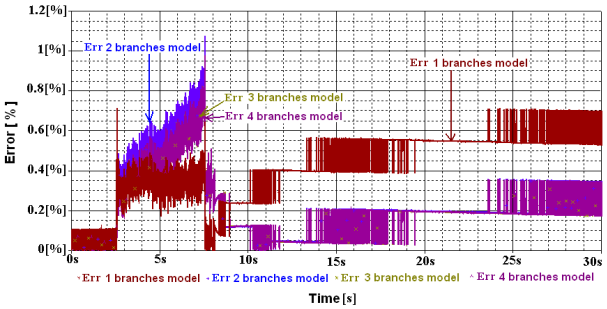

Fig. 17. Organic SC: Error analysis.

From the error analysis (Fig. 17) it can be identified that the 1 branch model of the organic SC has a 0.4 % error while modeling the rapid phenomena and 0.6 % error while modeling the relaxation process. The 2 branches model introduces high errors in the rapid phenomena modeling process (0.9 %). The 3 and 4 branches models have 0.8 % error while modeling the discharging process and 0.35 % error while modeling the relaxation process. Thus, to identify the optimal type of model that can be applied and to increase the accuracy of the modeling process, the process that is to be modeled has to be known.

The SC behavior depends on the electrolyte type. Moreover, the internal structure and the ions mobility of the inorganic SC does not allow to directly use the implemented model of the organic SC, in this case the error between the simulation and experiments for the 1 branch model being of 14 % both for the discharging and relaxing processes. To reduce the error between simulation and experiment, a compensation factor for the capacitance value was experimentally identified.

Also, the mobility of the hydrolyzed ions varies with temperature, thus influencing the behavior and the performances of the SC. These become critical especially at positive extreme temperatures (> 70 ^{o}C for organic SC and > 80 ^{o}C for inorganic SC) and extreme low temperatures (< -30 ^{o}C for organic SC and < - 40 ^{o}C for inorganic SC).

Experimentally has been demonstrated that the capacitance of the SC is directly proportional with temperature, the available energy increasing at high temperatures (Fig. 12). In contrast, the *ESR* value is decreasing while the temperature increases (Fig. 11). Thus, the inorganic SC developed model for + 25 ^{o}C was compensated by increasing the capacitance for experiments made at high temperatures and decreasing it for experiments made at low temperatures with a compensation factor determined with (10).

$$C_{dln} = C_{dln}+C_{dln+1}\cdot(T_{test} - T_{25^oC}) / 100 \quad (10)$$

where: T_{test} – test temperature; T_{25oC} – nominal temperature.

The results of the experiments vs. simulation of the model implemented for the 14 V/40F inorganic ECOND SC tested at + 25 ^{o}C are illustrated in Fig. 18 and the error between the model and experiments in Fig. 19.

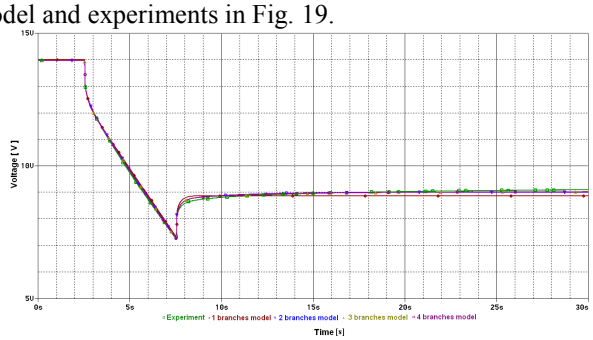

Fig. 18. Inorganic SC: Simulation vs. Experiment.

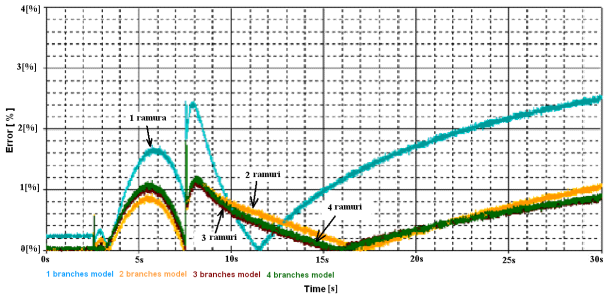

Fig. 19. Inorganic SC: Error analysis.

As it can be seen in Fig. 19, the 2, 3 and 4 branches models are more accurate (0.9 % error for 4 branches models) than the 1 branch model (2.5 %).

By interpreting the error analysis it can be identified that the rapid processes can be modeled with minimum error (0.8 %) by the 2 branches model and the slow processes are modeled with minimum error (0.9 % ÷ 0.1 %) by the 3 and 4 branches models. A good compromise to model both rapid and slow phenomena is the 2 branches model, which introduces a 0.9 % error while modeling the rapid phenomena and a medium of 1 % while modeling the slow phenomena.

VI. VALIDATING THE MODEL

The validation process of the determined models for organic and inorganic SC was made by checking the following steps:

- The parameters determined experimentally were compared with the ones specified in the datasheet. The values were situated between the specified ranges.
- The comparative error analysis between the model obtained from the EIS experimental data and the DC charge/discharge experimental data proved that the error was situated in the admitted range (<1 %), thus validating the developed model for both organic and inorganic SC.

By interpreting the error analyses, it was identified that there was a difference between the two types of SC because of the electrolyte type. Thus, the necessity of adjusting the organic SC model and obtaining a new model, dedicated to the inorganic SC was identified. Because of the reduced errors between simulation and experiment (< 1 %) it can be confirmed that the developed models express with high accuracy the behavior of both types of SC in the processes of DC discharging and relaxing. In conclusion, the developed models can be successfully used in the process of characterizing and modeling the behavior of the SC. This can be helpful in a wide range of applications, while developing and sizing the devices and while implementing the proper control strategies for combined energy storage and generation devices used in automotive applications, especially in HEV and EV.

VII. CONCLUSIONS

Nowadays, to increase the energy efficiency of the EV and HEV, the behavior and the characteristics of the SGD have to be known. Also, in automotive field it is mandatory to implement embedded systems that facilitate the driving process. This can be made by predicting the energy status and taking decisions regarding the modality to supply an EV or HEV. The conceived models of supercapacitors are useful for identifying where their performances are maximum and where they can be used in order to increase the global efficiency of the final application.

The present paper presents the differences in behavior for organic and inorganic SC. These differences can be

identified while testing the SC with DC charge/discharge and EIS methods and while modeling their behavior.

In the present paper two types of SC were tested with EIS and DC charge/discharge procedures: 2.7 V/2600 F organic SC and 14 V/40 F inorganic SC. To identify the SC behavior, the corresponding electrical models were developed by identifying the specific electrical parameters (*ESR*, C_{dl}) from the EIS experiments. To validate the models, DC charge/discharge measurements were used.

From the experimental data and from the error analysis, a difference in behavior between organic and inorganic SC was identified. This appears because of the different internal structure and different electrolyte of the two types of SC. The behavior of the organic SC was more predictable and easier to be modeled. To adapt the organic SC model, a compensation factor was identified. Thus, the error between the simulations and experiments was reduced from 14 % to less than 2 %.

Also, the experiments proved that the inorganic SC are characterized by increased power density and small time constants, being useful in the case of high power applications, such as providing the peak current pulses from the starting process of the classical vehicles or of the EV and HEV. Instead, the organic SC are characterized by increased energy density, being suitable for the process of supplying the engine of the EV and HEV and in the process of supplying the auxiliary loads of the vehicles in order to increase the energy efficiency. Through the loads that can be supplied from the SC, the following can be mentioned: lights, windscreen wiper, HVAC system, radio, GPS system, nigh vision system.

Thus, it can be said that the range of applications with supercapacitors is wide, as they are able to complement the existing classic solutions for energy storage and generation.

ACKNOWLEDGMENT

The experiments were made with the support of COST Action 542 and IFSTTART – Institut français des sciences et technologies des transports, de l'aménagement et des réseaux.

REFERENCES

[1] A.M. Puşcaş, M.C. Carp, P.N. Borza, and I. Szekely, "Embedded intelligent structures for energy management in vehicles", *Second IFIP WG 5.5/SOCOLNET Doctoral Conference on Computing, Electrical and Industrial Systems DOCEIS2011*, Costa de Caparica, Portugal, February 2011, pp. 421-428.

[2] S. Rael, B. Davat, and F. Belhachemi, "Supercondensateurs a couche double electrique, principe de fonctionnement et comportament electrique", *Journees Electrotechniques du Club EEA*, *Cachan*, pp. 57-67, March 2002.

[3] S.W. Novis, and L. McCloskey, "Non-aqueous electrolytes for electrical storage devices", *Patent, Philadelphia*, US, 2005.

[4] V. Khomenko, E. Raymundo-Pinero, and F. Béguin, "Optimization of an asymmetric manganese oxide/activated carbon capacitor working at 2 V in aqueous medium", *Carbon*, vol. 153, pp. 183-190, 2006.

[5] J.R. Miller, "A brief history of supercapacitors", *Batteries & Energy Storage Technology*, BEST, 2007.

[6] F. Beguin, and E. Frackowiak, *Carbons for electrochemical energy storage and conversion systems*. Advanced Materials and technologies Series. CRC Press Taylor and Francisc Group: Philadelphia, USA, 2010, pp.8.

[7] H. Gualous, D. Bouquain, A. Berthon, and J.M. Kauffmann, "Experimental study of supercapacitor serial resistance and capacitance variations with temperature", *Journal of Power Sources*, vol. 123, 2003, pp. 86-93.

[8] R. Kötz, and M. Carlen, "Principles and applications of electrochemical capacitors", *Electrochimica Acta*, vol. 45, 2000, pp. 2483-2498.

[9] J.N. Marie-Francoise, H. Gualous, R. Outbib, and A. Berthon, "42V Power Net with supercapacitor and battery for automotive applications", *Journal of Power Sources*, vol. 143, 2005, pp. 275-283.

[10] A.I. Belyakov, "Asymetric electrochemical supercapacitors with aqueous electrolytes", *ESSCAP'08*, Roma, Italia, November 2008.

[11] E. Hirose, Y. Ito, S. Onishi, M. Iwai, T. Yamaguchi, I. Aoki, K. Moriyama, and Y. Hashimoto, "Electric double layer capacitor and method for manufacturing the same", *Application Patent* 0090122467, 2009.

[12] J. Chmiola, G. Yushin, Y. Gogotsi, C. Portet, P. Simon, and P.L. Taberna, "Anomalous increase in carbon capacitance at pore sizes less than 1 nanometer", *Science*, vol. 313, nr. 5794, 2006, pp. 1760-1763.

[13] M. Toupin, D. Belanger, I.R. Hill, and D. Quinn, "Performance of experimental carbon blacks in aqueous supercapacitors", *Journal of Power Sources*, vol. 140, 2005, pp. 203-210.

[14] J. Chimola, G. Yushin, R. Dash, and Y. Gogotsi, "Effect of pore size and surface area of carbide derived carbon son specific capacitance", *Journal of Power Sources*, vol. 158, 2006, pp. 765-772.

[15] E. Frackowiak, G. Lota, J. Machnikowski, C. Vix-Guterl, and F. Beguin, "Optimisation of supercapacitors using carbons with controlled nanotexture and nitrogen content", *Electrochimica Acta*, vol. 51, 2006, pp. 2209-2214.

[16] R. Kötz, M. Hahn, and R. Gallay, "Temperature behaviour and impedance fundamentals of supercapacitors", *Journal of Power Sources*, vol. 154, 2006, pp. 550-555.

[17] [9-BARSALI] S. Barsali, M. Ceraolo, M. Marracci, B. Tellini, "Frequency dependent parameter model of supercapacitor", *Measurement*, vol. 43, 2010, pp. 1683-1689.

[18] [108-ORAZEM] M.E. Orazem and B. Tribollet, "An integrated approach to electrochemical impedance spectroscopy", *Electrochimica Acta*, vol. 53, 2008, pp. 7360-7366.

[19] ***, IEC 62391- 1 ed1.0. *Fixed electric double-layer capacitors for use in electronic equipment – Generic specification*. 2006-04-10.

[20] ***, IEC 62391- 2 ed1.0. *Fixed electric double-layer capacitors for use in electronic equipment – Sectional specification. Electric power capacitors for power application.* 2006-04-10.

[21] ***, IEC 62391- 2-1. *Fixed electric double-layer capacitors for use in electronic equipment – Blank detail specification. Electric power capacitors for power application. Assessment level EZ*. ed1.0, 2006-04-10.

[22] A.M. Puşcaş, M.C. Carp, C.Z. Kertesz, P.N. Borza, and G. Coquery, "Thermal and voltage testing and characterization of supercapacitors and Batteries", *Book of Abstracts of the 12th International Conference on Optimization of Electrical and Electronic Equipment*, Brasov, vol. 4, pp. 125-132, May 2010.

[23] M.A. Sakka, H. Gualous, J.V. Mierlo, and H. Culcu, "Thermal modelling and heat management of supercapacitors modules for vehicle applications", *Journal of Power Sources*, vol. 194, 2009, pp. 581-587.

[24] O. Bohlen, J. Kowal, and D.U. Sauer, "Ageing behaviour of electrochemical double layer capacitors Part I. Experimental study and ageing model", *Journal of Power Sources*, vol. 172, 2007, pp. 468-475.

[25] O. Bohlen, J. Kowal, and D.U. Sauer, "Ageing behaviour of electrochemical double layer capacitors Part II. Lifetime simulation model for dynamic applications", *Journal of Power Sources*, vol. 173, 2007, pp. 626-632.

[26] [125-RAFIK] F. Rafik, H. Gualous, R. Gallay, A. Crausaz, A. Berthon, "Frequency, thermal and voltage supercapacitor characterization and modeling*", Journal of Power Sources*, vol. 165, 2007, pp. 928-934.

[27] F. Belhachemi, S. Raël, and B. Davat, "Supercapacitors electrical behaviour for power electronics application", *9th International Conference and Exhibition on Power Electronics and Motion Control – EPE PEMC*, Kosice, Slovakia, September 2000, pp. 195.

[28] L. Zubieta, and R. Bonert, "Characterization of Double Layer Capacitor (DLCs) for Power Electronics Application", *IEEE Transaction on Industry Applications*, vol. 36, 2000, pp.199.